

Supporting Information

Thermodynamic Consequences of Tyr to Trp Mutations in the Cation- π -Mediated Binding of Trimethyllysine by the HP1 Chromodomain

Mackenzie W. Krone,^{†,‡} Katherine I. Albanese,^{†,‡} Gage O. Leighton,[¶] Alex J. Guseman,[†] Cyndi Qixin He,[§] Ga Young Lee,[§] Marc Garcia-Borràs,[§] Alex J. Guseman,[†] David C. Williams, Jr.,^{#, &} K. N. Houk,[§] Eric M. Brustad,^{*, †} Marcey L. Waters^{*, †}

[†]Department of Chemistry, University of North Carolina at Chapel Hill, Chapel Hill, North Carolina 27599, United States

[§]Department of Chemistry and Biochemistry, University of California, Los Angeles, California 90095, United States

[¶]Department of Biochemistry and Biophysics, University of North Carolina at Chapel Hill, 120 Mason Farm Rd, Campus Box 7260 Chapel Hill, NC 27599

[#]Department of Pathology and Laboratory Medicine, University of North Carolina at Chapel Hill, Campus Box 7525, Brinkhous-Bullitt Building, Chapel Hill, NC 27599

[&]Lineberger Comprehensive Cancer Center, University of North Carolina at Chapel Hill, 50 West Drive, Chapel Hill, NC 27599

Table of Contents

| | |
|--|-----|
| Materials and General Methods..... | S2 |
| Cloning and DNA and Protein Sequences..... | S2 |
| Chromodomain Expression and Purification..... | S3 |
| Peptide Synthesis and Purification..... | S4 |
| Circular Dichroism (CD) of HP1 Mutants..... | S5 |
| Isothermal Titration Calorimetry (ITC) Binding Measurements..... | S5 |
| Protein Crystallography..... | S5 |
| X-ray Data Collection and Protein Structure Determination..... | S6 |
| Verification of the Y24W Mutation in Protein Structure..... | S6 |
| E_{int} Calculations of HP1-Y24W Structure..... | S6 |
| ^1H - ^{15}N HSQC NMR Experiments..... | S7 |
| Figure S1. Chromodomain Alignment..... | S7 |
| Figure S2. PyMOL Mutagenesis of Y24 and Y48 of HP1 Chromodomain..... | S8 |
| Figure S3. SDS-PAGE Analysis of Purified Trp Mutants..... | S8 |
| Figure S4. Circular Dichroism of Chromodomains..... | S9 |
| Figure S5. ITC Curves of H3K9me3 Binding to HP1 Trp Mutants..... | S10 |
| Table S1. Data Collection and Refinement Statistics for Crystal Structure..... | S11 |
| Figure S6. Whole Protein Overlay of Wild-Type HP1 with HP1-Y24W..... | S12 |
| Figure S7. Density Maps of HP1-Y24W Chromodomain..... | S12 |
| Figure S8. Measured Cation- π and van der Waals contacts..... | S13 |
| Table S2. Quantitative analysis of the HP1-Y24W crystal structure..... | S14 |
| Figure S9. Quantum Mechanical Calculations of HP1-Y24W..... | S15 |
| Figure S10. ^1H - ^{15}N HSQC Spectra of Wild-type HP1 and HP1-Y24W..... | S16 |
| Figure S11. ^{15}N Relaxation Dispersion profiles of binding site residues of wild-type and Y24W HP1..... | S18 |

Materials and General Methods

Oligonucleotides were obtained from Integrated DNA Technologies. Enzymes and reagents used for cloning were obtained from New England BioLabs Inc. All other chemical reagents and solvents were obtained from chemical suppliers (Acros, Fisher Scientific, or Sigma-Aldrich) and used without further purification. DNA sequencing was performed by Genewiz. Residues 1-15 of H3 with trimethyllysine at position 9 (Sequence: ARTKQTARK(Me)₃STGGKAY, denoted as H3K9me3) was synthesized on a Tetras peptide synthesizer using Fmoc protected amino acids and Rink Amide AM resin (P3 Biosystems). H3K9me3 peptides were purified by reverse-phase HPLC (Waters), and purity was assessed using an Agilent Rapid Resolution LC-MSD system. Wild type HP1 and Trp mutant chromodomains were recombinantly expressed in *E. coli* (BL21-DE3) and purified using Ni-NTA affinity and size exclusion chromatography (GE). For NMR experiments, wild type and mutant HP1 proteins were expressed in ¹⁵N-enriched M9 media. ¹H-¹⁵N heteronuclear single quantum coherence spectra (HSQC) were collected at 298 K on a Bruker Avance III HD spectrometer equipped with a cryogenic QCI probe for each HP1 variant both free and bound to H3K9me3 (1:1.2 ratio). ITC experiments were performed using a Microcal AutoITC200, and CD spectra were obtained using an Applied Photophysics Chirascan. X-ray diffraction data were collected at Southeast Regional Collaborative Access Team (SER-CAT) at the Advanced Photon Source (Argonne National Laboratory) using beamline 22-ID and a MAR300HS CCD detector. PHENIX was used to solve protein structures. All quantum chemical calculations were performed using *Gaussian 09*. All graphics on optimized structures were generated with *CYLview*.

Cloning and DNA and Protein Sequences

The *Drosophila* HP1 chromodomain gene (residues 17–76 and an N-terminal 6xHis-tag) was previously cloned into a pET11a vector using NdeI and BamHI restriction sites. Mutations of the tyrosine cage residues to tryptophan (Y24W and Y48W) were generated using QuikChange PCR methods.

HP1 wild-type DNA sequence:

```
CAT ATG AAA AAA CAC CAC CAC CAC CAC CAC GCC GAA GAG GAG GAG GAG  
GAG TAC GCC GTG GAA AAG ATC ATC GAC AGG CGG GTG CGC AAG GGA ATG  
GTG GAG TAC TAT CTG AAA TGG AAG GGC TAT CCC GAA ACT GAG AAC ACG  
TGG GAG CCG GAG AAC AAT CTC GAC TGC CAG GAT CTT ATC CAG CAG TAC  
GAG GCG AGC CGC AAG GAT TAA GGA TCC
```

HP1 wild-type Protein sequence:

```
MKKHHHHHHAAEEEEEEYAVEKIIDRRVRKGMVEYYLKWKGYPETENTWEPENNLDCQ  
DLIQQYEASRKD
```

HP1 Y24W DNA sequence:

```
CAT ATG AAA AAA CAC CAC CAC CAC CAC CAC GCC GAA GAG GAG GAG GAG  
GAG TGG GCC GTG GAA AAG ATC ATC GAC AGG CGG GTG CGC AAG GGA ATG  
GTG GAG TAC TAT CTG AAA TGG AAG GGC TAT CCC GAA ACT GAG AAC ACG
```


After expression, cultures were pelleted at 4500 RPM for 10 min and the supernatant was decanted. Cell pellets were then resuspended in 20 mL lysis buffer (50 mM Tris, pH 8, 150 mM NaCl, 30 mM imidazole, 0.25 mg/mL lysozyme, cOmplete EDTA-Free Protease Inhibitor Cocktail Tablets (Roche)). The resuspended pellet was incubated at 37°C with 225 RPM shaking for 30 min and cooled on ice for 5 min. Pellets were sonicated on ice for 15 min until the lysate appeared homogenous. Lysate was clarified by centrifugation (19,000 RPM, Sorvall SS-34 rotor) for 45 min. Supernatant was decanted and filtered through a 0.45 µM syringe filter.

The expressed chromodomains were first purified with Ni-affinity chromatography by loading filtered lysate onto an ÄKTAPurifier UPC 10 (GE) equipped with a HisTrap- 5mL HP column (GE). HP1 wild-type and mutants were eluted using a step gradient from 0 – 55 % Buffer B (A: 50 mM Tris, 150 mM NaCl, 30 mM imidazole, 2 mM DTT, pH 7.4 B: 50 mM Tris, 150 mM NaCl, 300 mM imidazole, 2 mM DTT, pH 7.4). Eluted fractions were pooled and concentrated with a 3 kDa Amicon Ultra-15 Centrifugal filter. The concentrated sample was purified by size exclusion chromatography using a Superdex 200 10/300 GL size exclusion column equilibrated in buffer containing 50 mM sodium phosphate, pH 8, 25 mM NaCl, 2 mM DTT. Eluted fractions were pooled, concentrated and run on SDS-PAGE (**Figure S3**) and ESI-LCMS to confirm identity.

Peptide Synthesis and Purification

Residues 1-15 of H3 with trimethylated lysine at position 9 (Sequence: ARTKQTARK(Me)₃STGGKAY, furthermore denoted as H3K9me₃) was synthesized on a Tetras peptide synthesizer using Fmoc protected amino acids and Rink Amide AM resin (P3 Biosystems). A tyrosine residue was placed at the C-terminus for concentration determination. The amino acid residues were activated with HBTU (O-benzotriazole-N, N, N', N',-tetramethyluronium hexafluorophosphate) and HOBt (N-hydroxybenzotriazole) in the presence DIPEA (diisopropylethylamine). 4 equivalents of the amino acid, HBTU, and HOBt were used for each coupling step, along with 8 equivalents of DIPEA. Two coupling cycles of 30 minutes were performed in N-methyl-2-pyrrolidone for each residue. Deprotections of Fmoc were carried out in 20% piperidine in DMF (dimethylformamide), twice for 15 minutes each. The resin was washed DMF before every deprotection and coupling cycle.

Trimethyllysine was incorporated into the H3 peptide by first coupling Fmoc-Lys(Me)₂-OH·HCl (from Anaspec) for 5 hours with HBTU/HOBt activation. 2 equivalents of dimethyllysine, HBTU, and HOBt were used, along with 4 equivalents of DIPEA. Immediately after coupling, the resin was washed with DMF, and the residue was further methylated in presence of 7-methyl-1,5,7-triaza-bicyclo[4.4.0]dec-5-ene (MTDB, 1.2 eq) and methyl iodide (10 eq) in DMF for 6 hours. The resin was washed with DMF and peptide synthesis was continued with aforementioned conditions.

Peptides were cleaved from the resin with 95:2.5:2.5 trifluoroacetic acid (TFA):water:triisopropylsilane for 4 hours. The TFA was evaporated and products were precipitated with cold diethyl ether. The resulting peptides were extracted with water and lyophilized. Crude peptide material were purified by reversed phase HPLC using a C18

XBridge 5 μM column (Waters) and a gradient of 0 to 40% B in 60 minutes, where solvent A was 95:5 water:acetonitrile, 0.1% TFA and solvent B was 95:5 acetonitrile:water, 0.1% TFA. The purified peptides were lyophilized, and identity was confirmed by ESI-LCMS. Prior to ITC and CD, the peptide stock was desalted and exchanged into water using a PD MidiTrap G-10 column from GE and lyophilized to a powder.

Circular dichroism (CD) of HP1 mutants

CD experiments were performed using an Applied Photophysics Chirascan. Spectra were obtained with 25 μM chromodomain in 10 mM sodium phosphate buffer, pH 7.4 at 20°C. All scans were corrected with buffer subtraction. The mean residue ellipticity (MRE) was calculated using eq 1, where θ is MRE, signal is CD signal, l is path length, c is protein concentration, and r is the number of amino acid residues. All spectra were measured using a quartz cuvette with a path length of 0.1 cm (**Figure S4A**). 1 mM of H3K9me3 peptide was incubated with protein samples for bound-peptide measurements. The MRE of the H3K9me3 peptide was subtracted from the MRE of the HP1-bound complex to remove the unbound peptide contribution to the spectra.

$$\theta = \frac{\text{signal}}{10 \cdot l \cdot c \cdot r} \quad (1)$$

Thermal denaturation experiments were performed using the same buffer and concentrations as described above. Measurements were taken between 20 and 80°C. The melting curves were normalized to show fraction folded (α), calculated using eq 2, where θ is the observed MRE, θ_D is the MRE for the fully denatured protein, and θ_F is the MRE for the fully folded protein (**Figure S4B**).

$$\alpha = \frac{(\theta - \theta_D)}{(\theta_F - \theta_D)} \quad (2)$$

Isothermal titration calorimetry (ITC) binding measurements

ITC experiments were performed by titrating H3K9me3 peptide (3-3.5 mM) into HP1 mutants (180-230 μM) in 50 mM sodium phosphate, pH 7.4, 150 mM NaCl, 2 mM TCEP at 25°C using a Microcal AutoITC200. Peptide and protein concentrations were determined by measuring absorbance at 280 nm on a Cary 100 UV/Vis Spectrophotometer (Agilent Technologies). Heat of dilution was accounted for by subtracting the endpoint ΔH value from each prior injection. Data was analyzed using the One-Site binding model supplied in Origin software. ITC experiments were performed in triplicate for each protein, and error of thermodynamic values was calculated from the standard deviation of the three runs. (**Figure S5**).

Protein Crystallography

HP1-Y24W protein was diluted to a concentration of 10 mg/mL and mixed with 8.6 mg/ml H3K9me3 (4:1 peptide:protein) in 10 mM potassium phosphate, pH 7, 2mM TCEP. Crystals were grown by sitting drop vapor diffusion at 4°C. Cryschem Plates (Hampton Research) were set up by mixing 1 μL of the protein-peptide dilution and 1 μL of reservoir solution. The reservoir solutions that yielded initial hits for HP1-Y24W were 0.1 M MES,

pH 5.5-6.5, 3.2-3.6 M (NH₄)₂SO₄. Crystals were harvested and flash-frozen in liquid nitrogen with no supplementary cryoprotectant necessary.

X-ray Data Collection and Protein Structure Determination

X-ray diffraction data were collected at Southeast Regional Collaborative Access Team (SER-CAT) at the Advanced Photon Source (Argonne National Laboratory) using beamline 22-ID and a MAR300HS CCD detector. Data were collected at 100 K. Diffraction data sets were integrated and scaled with the automated data processing software KYLIN provided by SER-CAT.^[1] Initial phases were determined by molecular replacement against the wild-type HP1 structure (PDB:1KNE)^[2] using Phenix Phaser.^[3] Refinement was accomplished by iterative cycles of manual model building with Coot and automated refinement using Phenix Refine.^[4] Model quality was assessed with the Phenix Validation tool. All of the protein structure figures and alignments were generated using PyMOL software (The PyMOL Molecular Graphics System, Version 2.0.6, Schrödinger LLC.). (Table S1).

The HP1 wild-type structure (PDB: 1KNE) was overlaid with the HP1-Y24W (PDB: 6MHA) structure. RMS values were calculated using the align feature of PyMOL. Alignment of wild-type and HP1-Y24W gave an RMSD of 0.19 Å (Figure S6A).

Verification of the Y24W Mutation in HP1-Y24W Protein Structure

For the HP1-Y24W structure, the first refinement was performed with the HP1 wild-type sequence. After refinement, the mFo-DFc map showed extra electron density around the tyrosine residue at the 24 position. When the tyrosine is mutated to tryptophan, the mFo-DFc density encompasses 24W. Once the Y24W mutation model is refined, the 2mFo-DFc density fits the tryptophan relatively well. Furthermore, the mFo-DFc density after refinement with 24W does not depict any extra electron density where the hydroxyl of the tyrosine residue in wild-type would be positioned (Figure S7C).

E_{int} calculations for HP1 and HP1-Y24W proteins with trimethyllysine

The geometries of the HP1–KMe₃ and the Y24W–KMe₃ complexes were extracted and truncated to include only the amino acid side chains from their corresponding crystal structures. Each terminus of the fragments was capped with a hydrogen atom at 1.09 Å. Electronic interaction energies, E_{int}, were calculated for each and all amino acids with the lysine ammonium ion using single-point energy calculations at the M06-2X/6-311+G(d,p) level of theory.^[5] M06-2X functional has previously shown to describe cation-π interactions accurately.^[6] The computed electronic interaction energy (E_{int}) is defined as the energy difference between the complex and substrate and amino acid: $E_{int} = E_{complex} - (E_{Kme3} + E_{AA})$. All quantum chemical calculations were performed using Gaussian 09.⁷ All graphics on optimized structures were generated with CYLview (Figure S9).⁸

E_{int} calculations for HP1-Y24W complex for additional CH-π interactions

The geometries of the side chains of W24 and KMe₃ were extracted and truncated from the crystal structure of HP1–Y24W complex. β-carbon of W24 side chain and KMe₃ terminus were capped with a hydrogen atom at 1.09 Å. The pentyl alkyl chain of the KMe₃

was successively truncated by removing one carbon at a time to generate 4 different models: $\text{Me}(\text{CH}_2)_n\text{NMe}_3^+$, where $n = 0-3$ (see scheme). Single point energy was calculated for each truncated dimer using M06-2X/6-311+G(d,p) level of theory.^[5] All quantum chemical calculations were performed using Gaussian 09.^[7] All graphics on optimized structures were generated with CYLview (**Figure S9**).^[8]

NMR Experiments

Uniformly $^{15}\text{N}(\pm^{13}\text{C})$ -labeled wild-type and mutant HP1 proteins were expressed in BL21(DE3) and grown in 1L of $^{15}\text{N}(\pm^{13}\text{C})$ -enriched M9 media. The bacteria were grown to an OD_{600} of ~ 0.6 at 37°C , expression induced with 0.1 mM IPTG (Fisher), and cultures incubated at 18 overnight.

$^{15}\text{N}(\pm^{13}\text{C})$ -labeled purified proteins (250 μM) were exchanged into NMR buffer (20 mM sodium phosphate pH 7.5 (95/5 $\text{H}_2\text{O}/\text{D}_2\text{O}$)) and H3K9me3 added (300 μM) for peptide bound experiments at a 1:1.2 protein:peptide molar ratio (**Figure 5, S10**). All two- and three-dimensional NMR spectra were collected at 298 K on a Bruker Avance III spectrometer equipped with a cryogenic QCI probe and operating at a ^1H frequency of 500, 700, or 850 MHz. Data was processed using the NMR-Pipe program^[9] and analyzed using the CcpNMR Analysis software^[10].

The HP1 backbone resonances were assigned for uniformly $^{15}\text{N},^{13}\text{C}$ -labeled protein based on three-dimensional heteronuclear spectra (HNCO, HNCA, CBCA(CO)NH, and HNCACB) following standard methods. The resonance assignment data have been deposited in the Biological Magnetic Resonance Bank (BMRB ID: 28060). The assignments were propagated to the HP1-Y24W and peptide bound complexes based on comparison of ^{15}N -HSQC spectra and serial titration experiments.

Relaxation dispersion

Relaxation dispersion spectra were collected at 500, 700, and 850 MHz with a 60 ms CPMG constant time delay.^[11] A total of 13 pulse frequencies (ν_{CPMG}), ranging from 67 to 1800 Hz with a repeat of two frequencies for error analysis, were collected and analyzed as described previously^[12] using the relax-nmr software^[13].

| | | 24 | 45 | 48 | |
|--------|------|--------------------|-----------------------|-------------------|-----------------|
| 1KNE:A | HP1 | EEEEEEYAVEKI | IDRRVVRKGMVEY | YLLKWKGY | PETENTWEPENNLDC |
| 3FDT:A | CBX5 | --- | GEEYVVEKVLDRRVVKGQVEY | LLKWKGF | SEEHNTWEPEKNLDC |
| 2L11:A | CBX3 | ---- | GEFVVEKVLDRRVVNGKVEY | FLKWKGF | TDADNTWEPEENLDC |
| 3F2U:A | CBX1 | ---- | GEYVVEKVLDRRVVKGKVEY | LLKWKGF | SDEDNTWEPEENLDC |
| 1PDQ:A | dPC | DPVDLVYAAEKI | IQRVKKGVVEYRVKWK | GNQRYNTWEPEVNILD | |
| 4MN3:A | CBX7 | --GEQVFAVESIRK | KRVKGVVEYLVKWK | GWPPKYSTWEPEEHILD | |
| 5EPK:A | CBX2 | --GEQVFAAECILSKRLR | KGKLEYLVKWRG | WSSKHNSWEPEENILD | |
| 5EPL:A | CBX4 | -GSEHVFAVESIEK | KRIRKGRVEYLVKWRG | WSPKYNTWEPEENILD | |
| 3I91:A | CBX8 | ---ERVFAAEALLKRR | IRKGRMEYLVKWK | GSQKYSTWEPEENILD | |
| 3I90:A | CBX6 | ----RVFAAESIIKRR | IRKGRIEYLVKWK | GWAIKYSTWEPEENILD | |

Figure S1. Alignment of *Drosophila* and mammalian HP1 and polycomb (dPC) chromodomains. Aromatic cage recognition motif highlighted in blue; aromatic residues

corresponding to Y24 and W45 are highly conserved across HP1 and polycomb chromodomains.

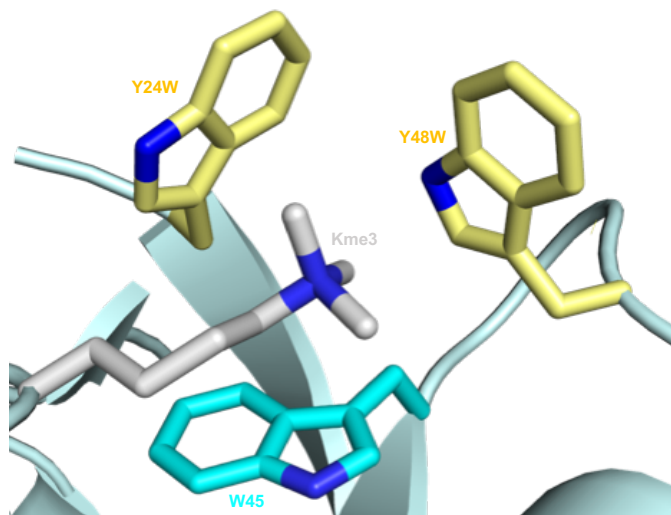


Figure S2. PyMOL mutagenesis of Y24 and Y48 of HP1 chromodomain. As a qualitative measure of steric clash, Y24 and Y48 were mutated to Trp in the wild-type HP1 chromodomain crystal structure (PDB ID: 1KNE). The most statistically likely backbone dependent Trp rotamers (36.7% for Y24W and 56.3% for Y48W) based on PDB structures showed minimal VDW clash. Both predicted rotamers are shown in yellow within the wild-type structure.

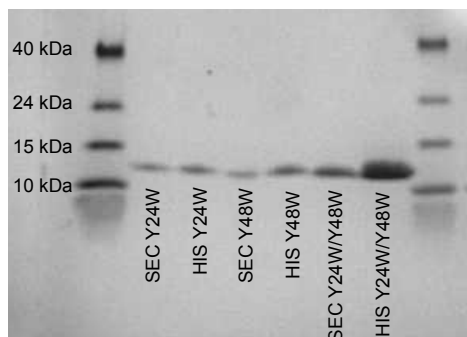


Figure S3. SDS-PAGE analysis of purified Trp mutants. 6xHis-Tagged purification followed by size exclusion chromatography (SEC) purification of HP1 Trp mutants.

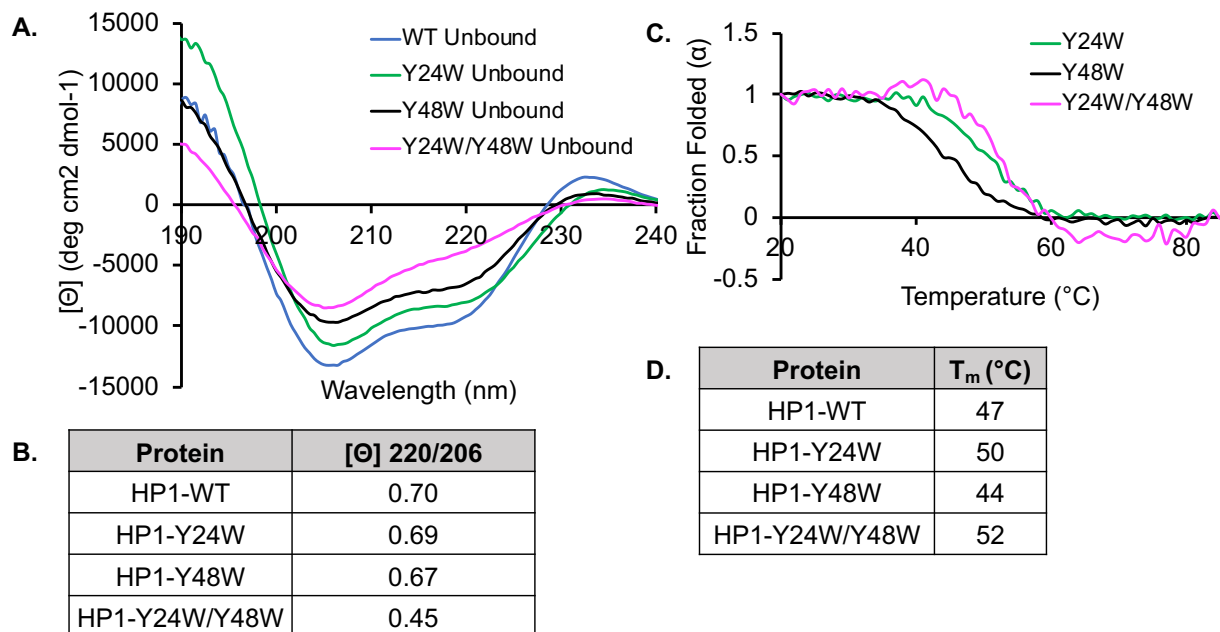


Figure S4. Circular dichroism of HP1 wild type and Trp chromodomains. (A) CD spectra of HP1 chromodomains in 10 mM sodium phosphate, pH 7.4. (B) Ratio of MRE (θ) values at 220 and 206 nm; there are no significant differences in the degree of folding for the single mutants and wild type HP1, however the double mutant does appear to be less well folded. (C) Thermal melt (T_m) curves of HP1 Trp mutants in 10 mM sodium phosphate, pH 7.4. (D) T_m of wild-type HP1^[14] and Trp mutants; the mutations do not significantly affect the overall stability of the chromodomain.

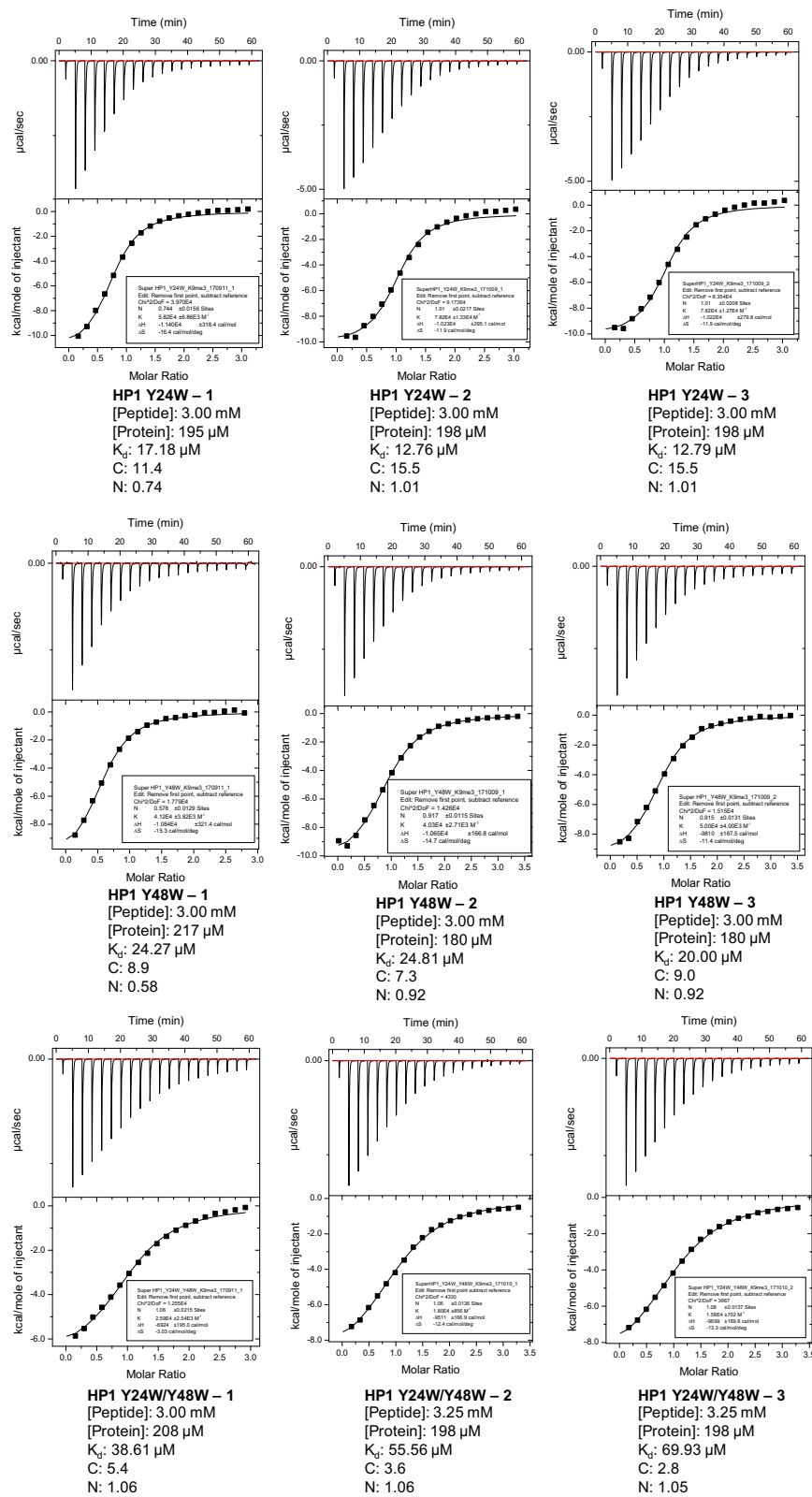


Figure S5. ITC curves of H3K9me3 binding to HP1 Trp mutants.

Table S1. Data collection and refinement statistics for HP1-Y24W chromodomain.

| HP1-Y24W | |
|---|---------------------|
| PDB accession # | 6MHA |
| Data collection | |
| Space group | C 2 2 21 |
| Wavelength | 1.000 |
| Cell dimensions | |
| <i>a</i> , <i>b</i> , <i>c</i> (Å) | 34.01, 76.70, 76.51 |
| <i>a</i> , <i>b</i> , <i>g</i> (°) | 90.00, 90.00, 90.00 |
| Resolution (Å) | 1.52 (1.55-1.51) |
| <i>R</i> _{merge} | 3.8 (28.2) |
| <i>I</i> / <i>σ</i> | 27.1 (2.9) |
| Completeness (%) | 97.2 (48.9) |
| Redundancy | 6.6 (2.5) |
| Refinement | |
| Resolution (Å) | 1.52 |
| No. reflections | 30,105 |
| <i>R</i> _{work} / <i>R</i> _{free} | 0.19 / 0.22 |
| No. atoms | |
| Protein | 477 |
| Ligand/ion | 49 |
| Water | 34 |
| <i>B</i> -factors | |
| Protein | 27.6 |
| Ligand/ion | 31.9 |
| Water | 36.8 |
| R.m.s deviations | |
| Bond lengths (Å) | 0.013 |
| Bond angles (°) | 1.317 |
| Ramachandran outliers (%) | 0 |

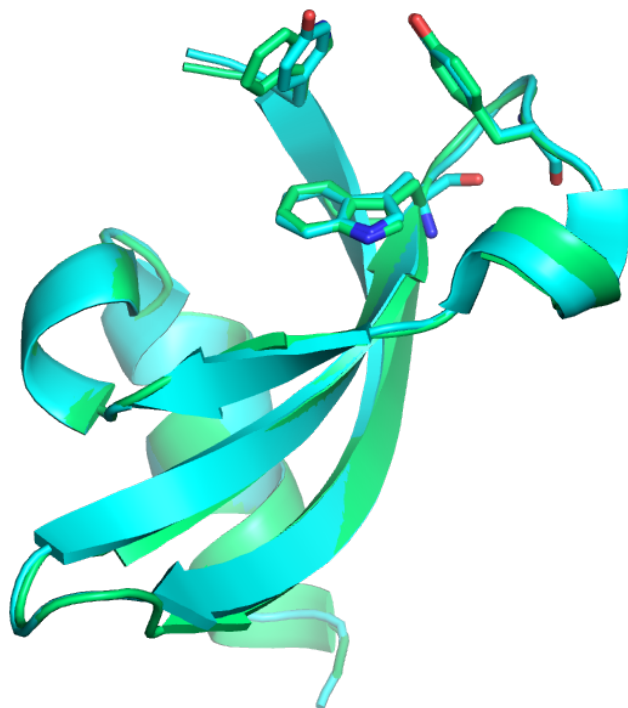


Figure S6. Full structure overlay of HP1-Y24W (green) with the wild-type chromodomain (cyan).

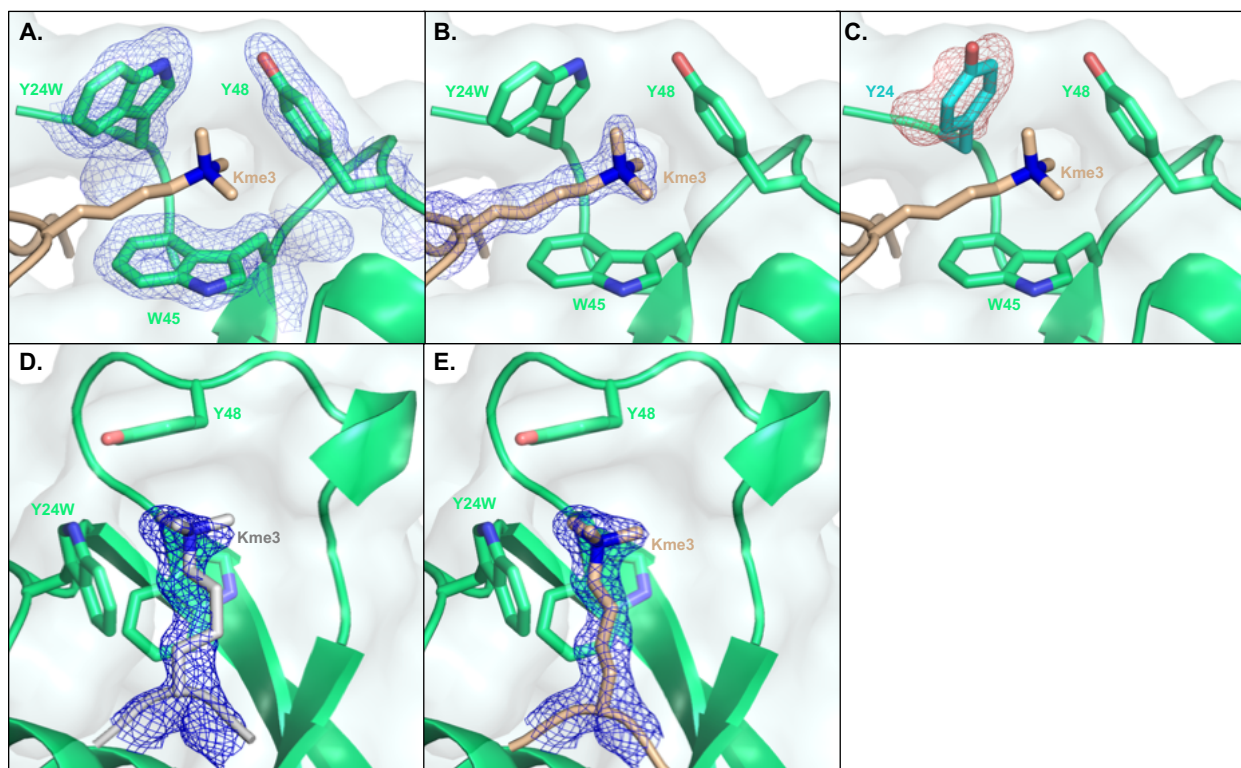


Figure S7. Density maps of HP1-Y24W chromodomain. (A) 2mFo-DFc map of Y24W, Y48, W45, and (B) Kme3 ligand. (C) mFo-DFc map of Y24W density with Y24 shows additional density for Trp at that position. (D) 2mFo-DFc map of HP1-Y24W Kme3 density

with wild-type Kme3. (E) 2mFo-DFc map of HP1-Y24W Kme3 density shows that the ligand in the HP1-Y24W structure is in an anti conformation unlike the gauche wild type conformation, which does not fit the density well. All maps are contoured at 1.5 σ .

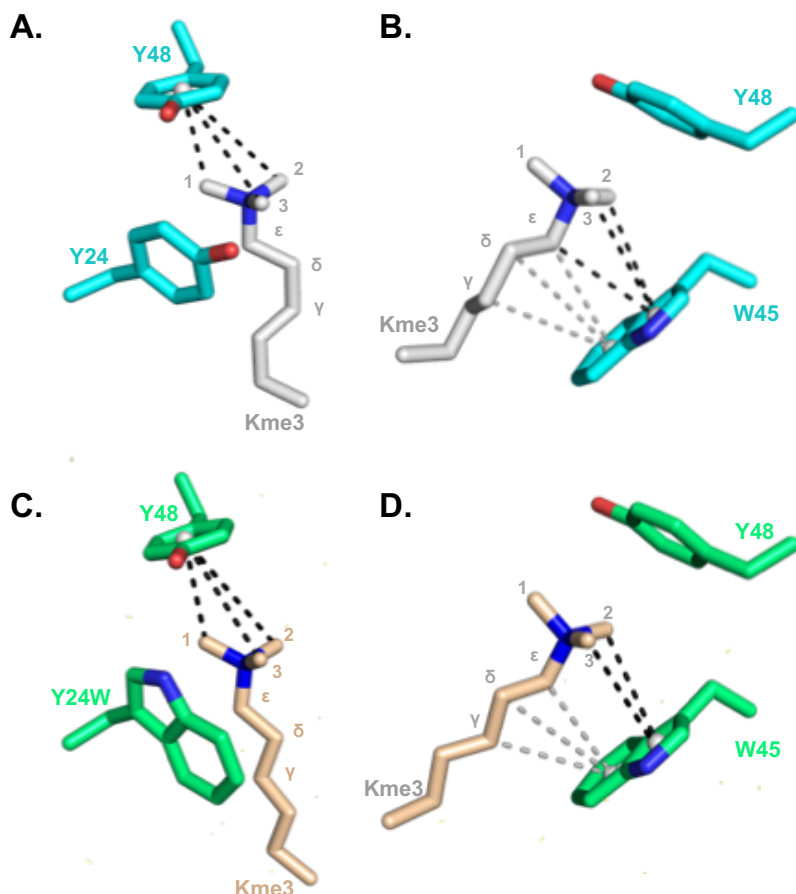


Figure S8. Measured cation- π (black) and van der Waals (grey) contacts between Kme3 N-methyls and methylenes to aromatic cage residues. (A, B) HP1 wild-type contacts between H3K9me3 and (A) Y48 and (B) W45. (C, D) HP1-Y24W contacts between H3K9me3 and (C) Y48 and (D) W45. Corresponding distance measurements from N-methyls and methylenes are located in Table S2.

Table S2. Qualitative analysis of HP1-Y24W crystal structure. Distances measured between the centroid of each aromatic ring with respect to Kme3 N-methyl groups and the methylenes of the Kme3 alkyl side chain.

| | Distance (Å) | | | | | |
|------------------|-------------------|-------------------|-------------------|-------------------|-------------------|-------------------|
| | CH ₃ 1 | CH ₃ 2 | CH ₃ 3 | CH ₂ γ | CH ₂ δ | CH ₂ ε |
| Wild Type | | | | | | |
| Y24 | 3.6 | 4.0 | - | 5.5 | 4.9 | 4.1 |
| Y48 | 4.6 | 3.3 | 4.5 | - | - | 5.3 |
| W45, 5 mem | - | 4.0 | 4.5 | 5.2 | 4.9 | 3.9 |
| W45, 6 mem | - | 4.8 | 5.7 | 4.8 | 5.1 | 4.1 |
| HP1-Y24W | | | | | | |
| Y24W, 5 mem | 3.8 | 4.0 | - | 5.4 | 5.0 | 4.2 |
| Y24W, 6 mem | 3.9 | 4.9 | - | 4.4 | 4.1 | 4.0 |
| Y48 | 4.6 | 3.5 | 4.7 | - | - | 5.8 |
| W45, 5 mem | - | 4.0 | 4.1 | 5.0 | 4.9 | 3.9 |
| W45, 6 mem | - | 4.4 | 5.1 | 4.1 | 4.5 | 3.7 |

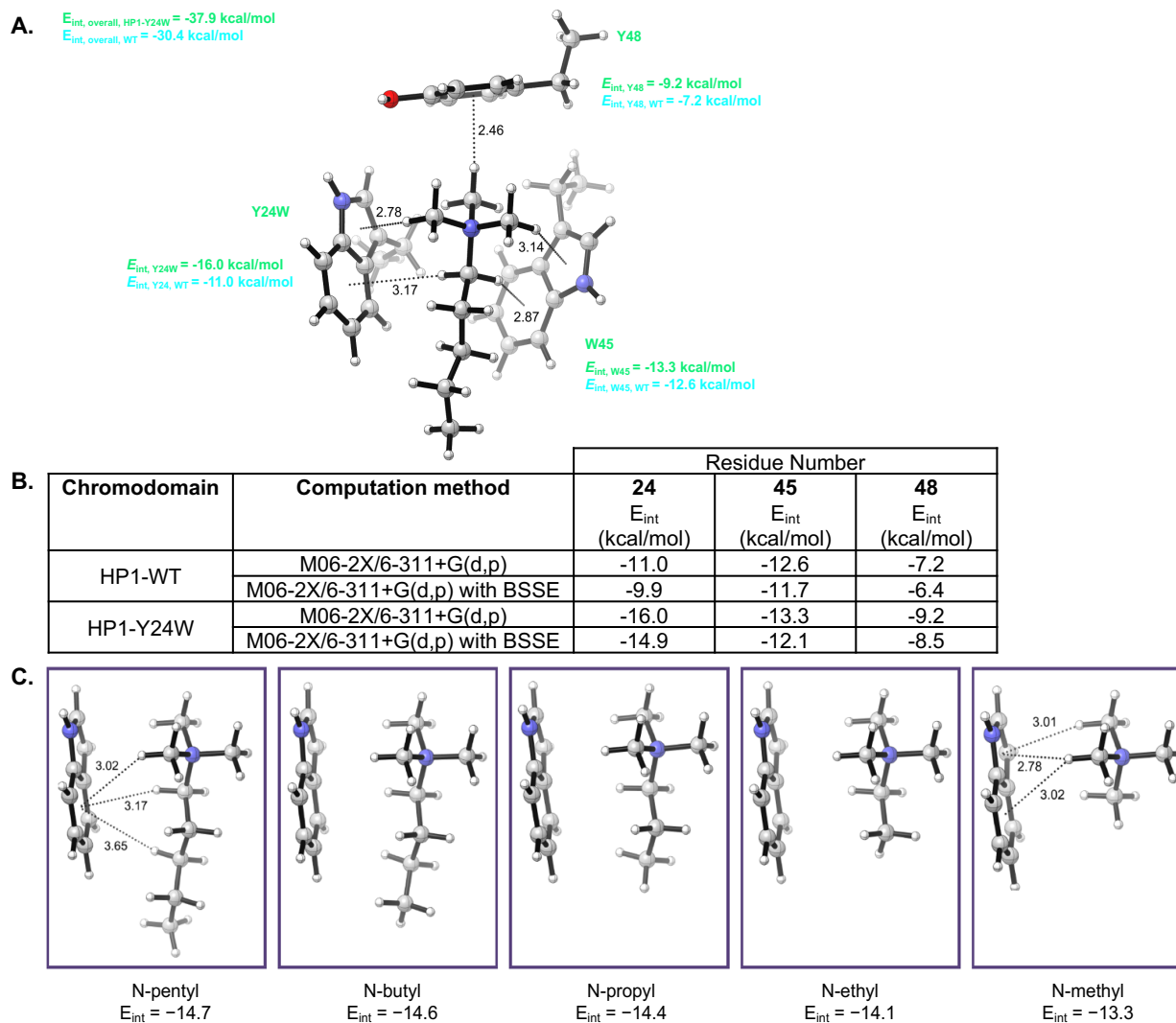
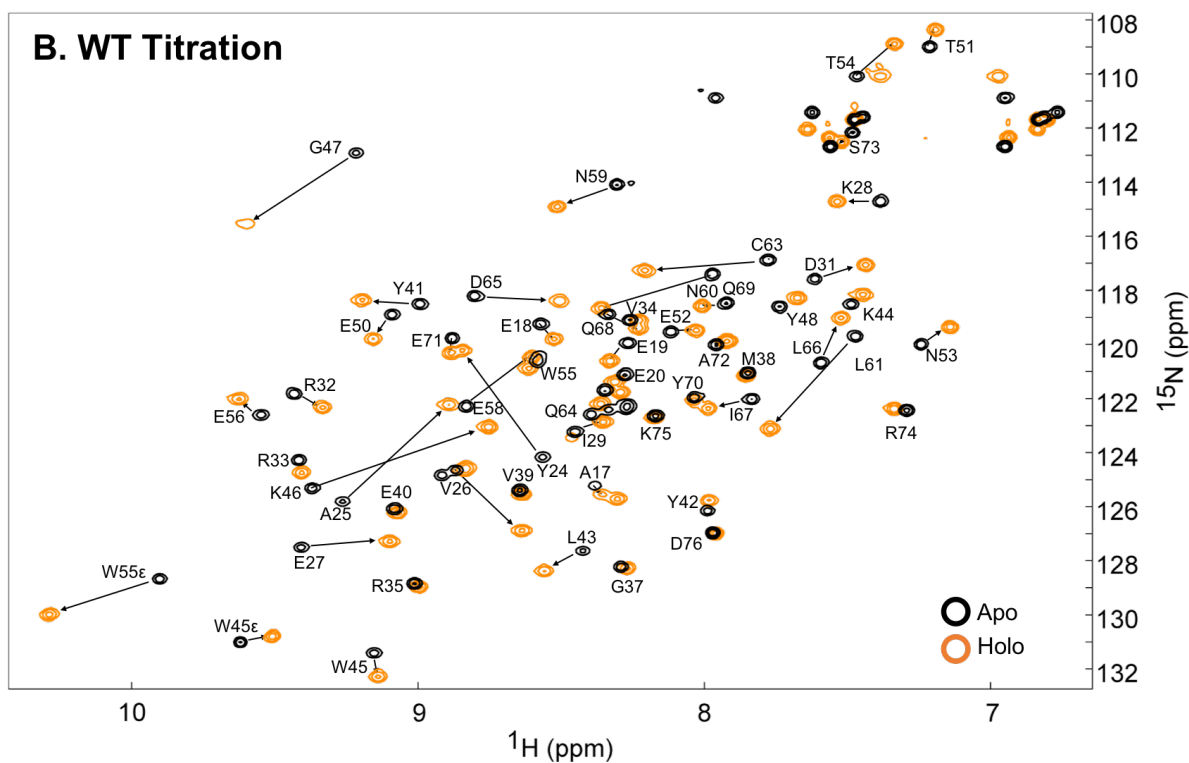
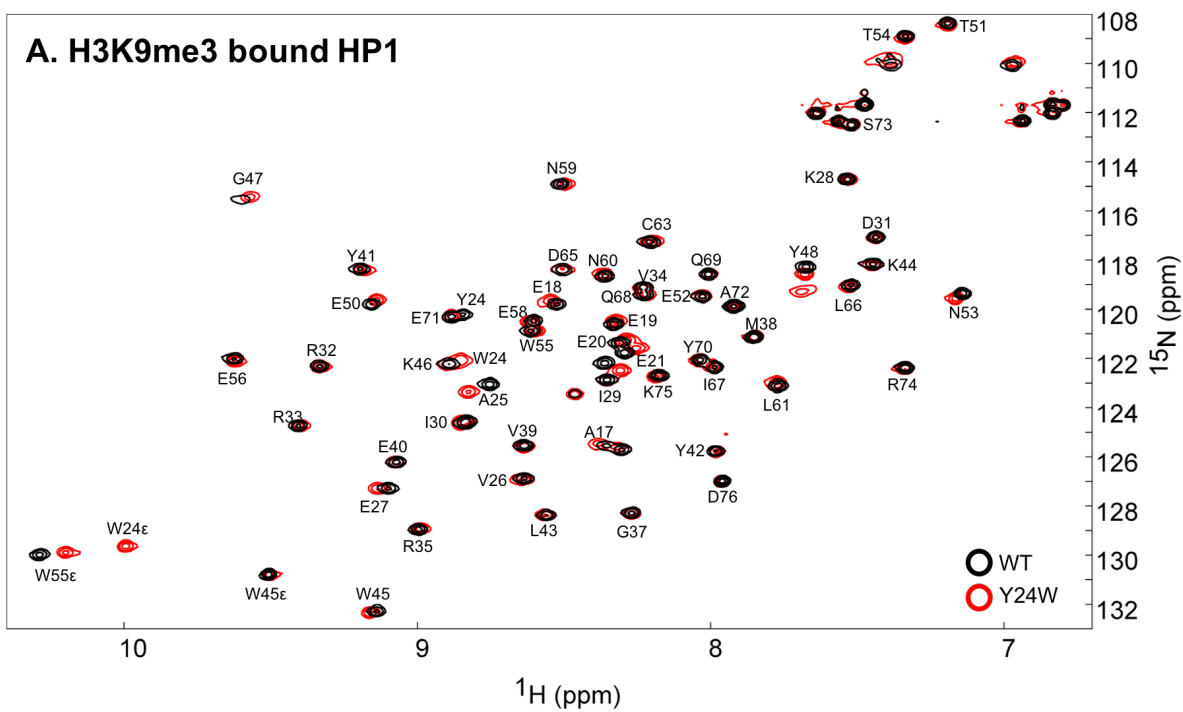


Figure S9. Quantum mechanical calculations of HP1 wild-type and HP1-Y24W chromodomain. Calculations were completed at the M06-2X/6-311+G(d,p) level of theory. (A) Interaction energies (E_{int}) where $E_{\text{int}} = E_{\text{complex}} - (E_{\text{Kme3}} + E_{\text{a.a. sidechain}})$ were calculated directly from the wild-type (cyan) and HP1-Y24W (green) crystal structures to determine the E_{int} for each residue with Kme3 and the E_{int} for the overall complex. (B) Comparison of E_{int} for each residue calculated with and without basis set superposition error (BSSE). BSSE makes 0.8 to 1.2 kcal/mol difference to each E_{int} , but the relative E_{int} trends are consistent and agree well with experimental ΔH . (C) Contribution of the pentyl alkyl chain to the stabilization of Kme3 in the HP1 chromodomain. E_{int} for the HP1-Y24W:Kme3 interaction was calculated for each successive truncation of the Kme3 side chain.



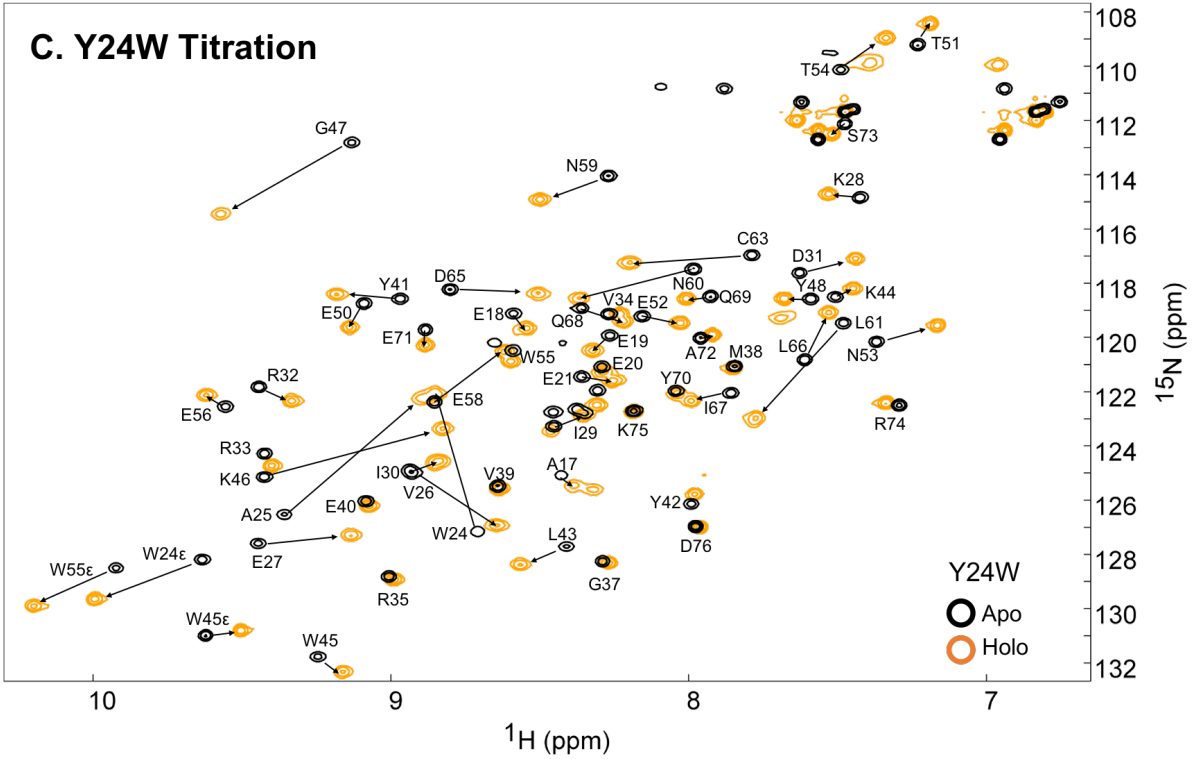
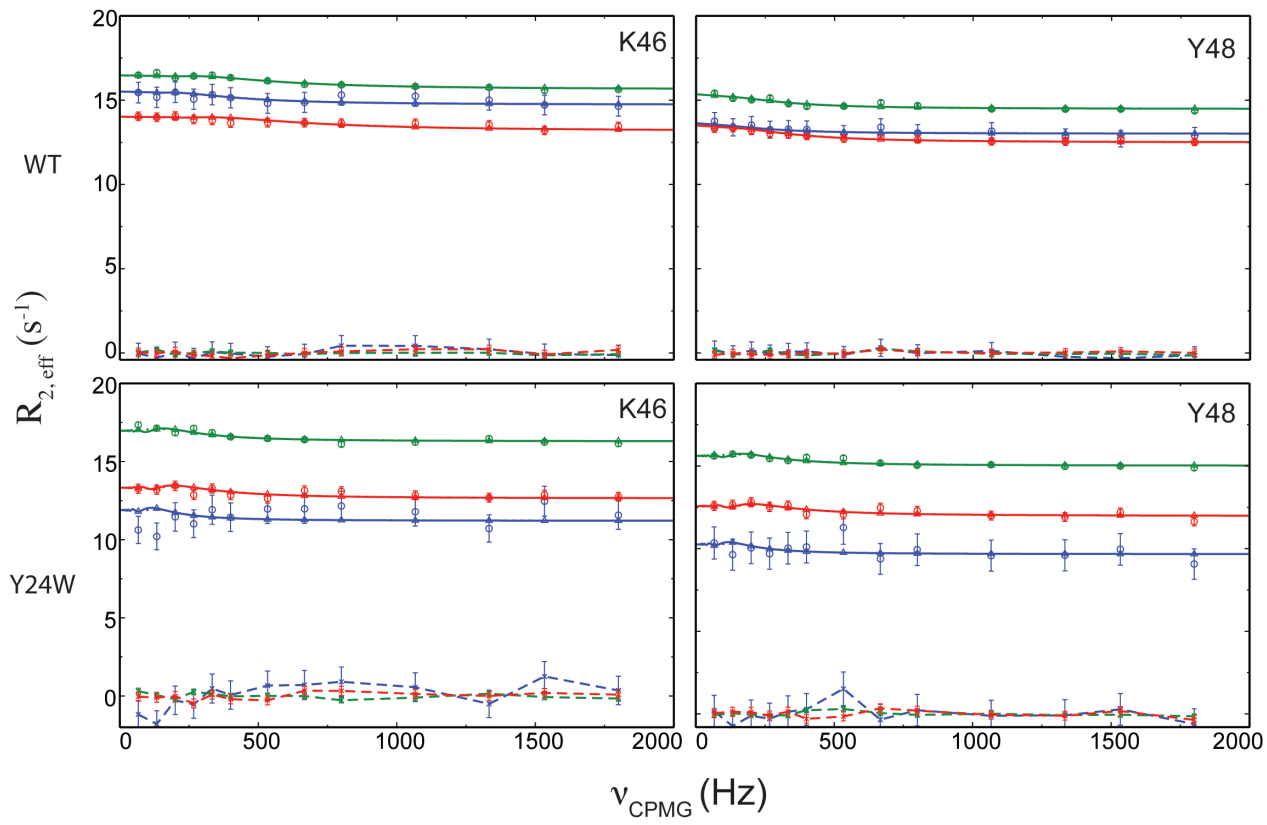
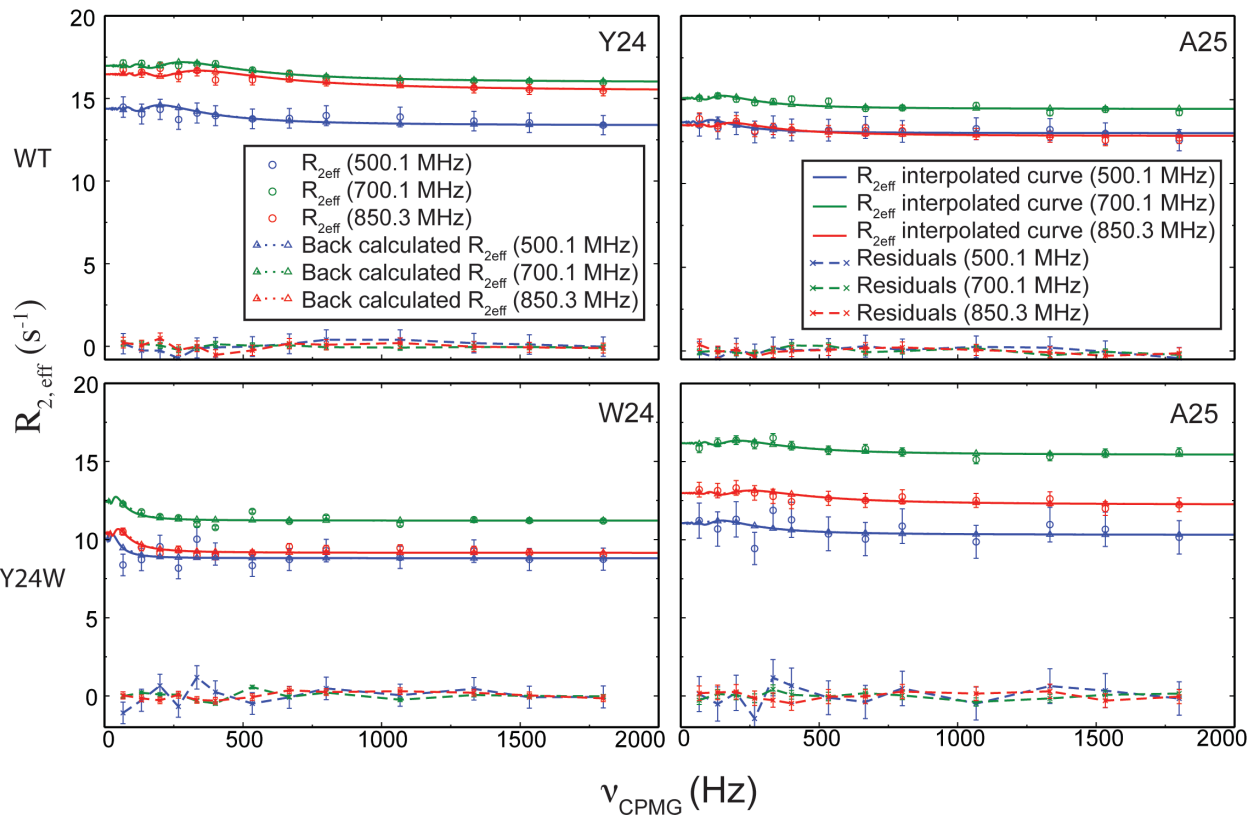
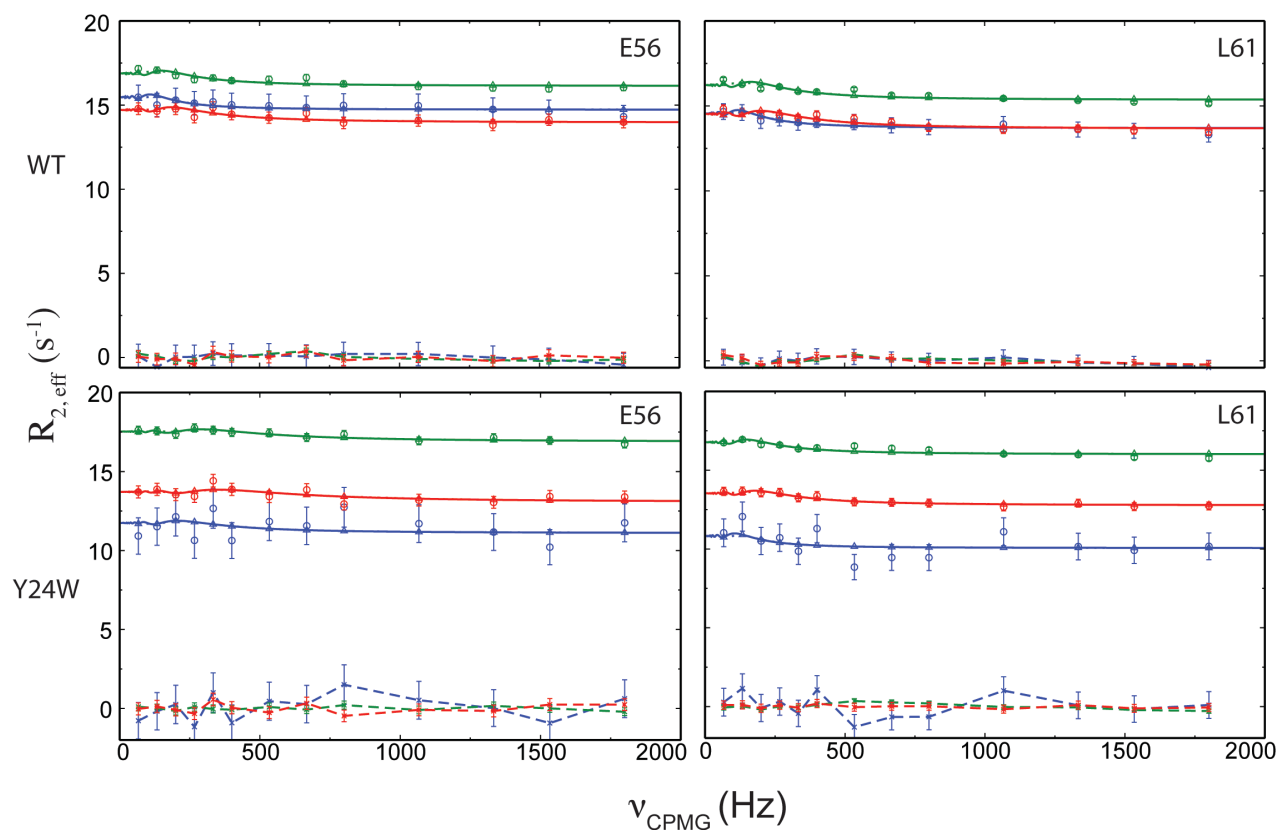


Figure S10. (A) ^1H - ^{15}N HSQC spectra of wild-type HP1 (black) and HP1-Y24W (red) bound to H3K9me3 have very minimal chemical perturbations indicating conserved protein folds. HSQC overlay of WT HP1 (B) or Y24W (C) in the apo (black) and holo (orange) states.





S11. ^{15}N Relaxation Dispersion profiles of binding site residues of wild-type or Y24W HP1. Selected residues surrounding the binding site are shown. RD curves (solid lines) are remarkably similar between proteins indicating that there is no difference in protein dynamics on the millisecond timescale.

- [1] Z.-Q. Fu, *Acta Crystallographica Section D Biological Crystallography* **2005**, *61*, 1643-1648.
- [2] S. A. Jacobs, S. Khorasanizadeh, *Science* **2002**, *295*, 2080-2083.
- [3] P. D. Adams, P. V. Afonine, G. Bunkóczi, V. B. Chen, I. W. Davis, N. Echols, J. J. Headd, L.-W. Hung, G. J. Kapral, R. W. Grosse-Kunstleve, A. J. McCoy, N. W. Moriarty, R. Oeffner, R. J. Read, D. C. Richardson, J. S. Richardson, T. C. Terwilliger, P. H. Zwart, *Acta crystallographica. Section D, Biological crystallography* **2010**, *66*, 213-221.
- [4] P. Emsley, B. Lohkamp, W. G. Scott, K. Cowtan, *Acta Crystallographica Section D Biological Crystallography* **2010**, *66*, 486-501.
- [5] Y. Zhao, D. G. Truhlar, *Theoretical Chemistry Accounts* **2008**, *120*, 215-241.
- [6] M. R. Davis, D. A. Dougherty, *Phys. Chem. Chem. Phys.* **2015**, *17*, 29262-29270.
- [7] G. W. T. M. J. Frisch, H. B. Schlegel, G. E. Scuseria, M. A. Robb, J. R. Cheeseman, G. Scalmani, V. Barone, G. A. Petersson, H. Nakatsuji, X. Li, M. Caricato, A. Marenich, J. Bloino, B. G. Janesko, R. Gomperts, B. Mennucci, H. P. Hratchian, J. V. Ort, *Gaussian, Inc.* **2016**.
- [8] C. Y. C. Legault, *Université de Sherbrooke* **2009**, *version 1*.
- [9] F. Delaglio, S. Grzesiek, G. W. Vuister, G. Zhu, J. Pfeifer, A. Bax, *J Biomol NMR* **1995**, *6*, 277-293.
- [10] W. F. Vranken, W. Boucher, T. J. Stevens, R. H. Fogh, A. Pajon, M. Llinas, E. L. Ulrich, J. L. Markley, J. Ionides, E. D. Laue, *Proteins* **2005**, *59*, 687-696.
- [11] aJ. Patrick Loria, Mark Rance, ‡ and, Arthur G. Palmer III*, **1999**; bDong Long, a. Maili Liu, Daiwen Yang*, **2008**.
- [12] M. J. Sperlazza, S. M. Bilinovich, L. M. Sinanan, F. R. Javier, D. C. Williams, *J Mol Biol* **2017**, *429*, 1581-1594.
- [13] aE. J. d'Auvergne, P. R. Gooley, *J Biomol NMR* **2008**, *40*, 121-133; bE. J. d'Auvergne, P. R. Gooley, in *J Biomol NMR, Vol. 40*, **2008**, pp. 107-119.
- [14] R. J. Eisert, S. A. Kennedy, M. L. Waters, *Biochemistry* **2015**, *54*, 2314-2322.